Development 133, 1811-1821 (2006) doi:10.1242/dev.02351

The level of sonic hedgehog signaling regulates the complexity of cerebellar foliation

JoMichelle D. Corrales[1,2,*], Sandra Blaess[1,2], Eamonn M. Mahoney[1] and Alexandra L. Joyner[1,2,3,†]

Foliation of the mouse cerebellum occurs primarily during the first 2 weeks after birth and is accompanied by tremendous proliferation of granule cell precursors (GCPs). We have previously shown that sonic hedgehog (Shh) signaling correlates spatially and temporally with fissure formation, and that Gli2 is the main activator driving Shh induced proliferation of embryonic GCPs. Here, we have tested whether the level of Shh signaling regulates the extent of cerebellar foliation. By progressively lowering signaling by removing Gli1 and Gli2 or the Shh receptor smoothened, we found the extent of foliation is gradually reduced, and that this correlates with a decrease in the duration of GCP proliferation. Importantly, the pattern of the remaining fissures in the mutants corresponds to the first fissures that form during normal development. In a complementary manner, an increase in the level and length of Shh signaling results in formation of an extra fissure in a position conserved in rat. The complexity of cerebellar foliation varies greatly between vertebrate species. Our studies have uncovered a mechanism by which the level and length of Shh signaling could be integral to determining the distinct number of fissures in each species.

KEY WORDS: Gli1, Gli2, Gli3, Shh, Cerebellum, Patterning, Mouse

INTRODUCTION

The relatively few well-defined cell types within the cerebellum and the stereotypical foliation pattern make the cerebellum particularly amenable to the study of morphogenesis in the central nervous system (CNS). The mammalian cerebellum consists of a central vermis and two lateral hemispheres, each with its own sets of fissures. The complexity of the foliation pattern varies between species of mammals, depending on the proprioceptive input to the cerebellum. For example, the cerebellar vermis of many inbred mouse strains consists of eight major lobules with few sublobules, whereas the rat vermis consists of ten lobules and contains more sublobules. Furthermore, some inbred strains of mice have one or two additional partial lobules corresponding to additional lobules in rat. Although the basic ten lobules present in the rat are conserved in human, each human cerebellar lobule is extensively subdivided into many sublobules. The conservation of morphology within and across species suggests that patterning of cerebellar folia is genetically regulated. An important question is what factors determine the degree of foliation in different species.

Foliation of the rodent cerebellum is generated in distinct phases (Altman and Bayer, 1997). First, the smooth cerebellar surface is divided into five cardinal lobes by four principle fissures in the vermis (see Fig. 8). Next, the process of lobulation divides the cardinal lobes into the individual lobules present in the adult cerebellum. Some of the lobules are then further subdivided into sublobules, and finally each lobule grows to a specific size. In the mouse and rat, the emergence of the five cardinal lobes is observed by birth. The foliation pattern elaborates for 2 weeks after birth in mouse and 3 weeks in rat. Although a number of theories have been proposed (Lauder et al., 1974; Mares and Lodin, 1970), it remains unknown how the conserved position of the fissures is determined, and what genetic mechanisms regulate the size and complexity of the lobes. It is also not known whether positioning of the folia and regulation of the number of fissures are independent or inter-related events.

The cerebellum undergoes over a 1000-fold increase in volume during development (Goldowitz et al., 1997). Postnatally, this is largely due to the proliferation of the GCPs and occurs simultaneously with the formation and growth of the folia. The generation of granule cells and the process of cerebellar growth and foliation appear to be related, as mice or rats in which the granule cell population is compromised develop smaller cerebella with reduced foliation (Aruga et al., 1998; Doughty et al., 1998; Dussault et al., 1998). GCP proliferation is dependent on interactions with Purkinje cells (PCs), as demonstrated by the observed decrease in granule cell number when PCs are lost because of cell ablation or genetic mutation (Caddy and Biscoe, 1979; Herrup, 1983; Sidman et al., 1962; Smeyne et al., 1995; Wetts and Herrup, 1982).

A number of lines of evidence suggest the mitogenic effect of PCs on granule cells is mediated by sonic hedgehog (Shh), a secreted factor expressed in PCs from E17.5 onwards in the mouse. First, Shh increases and sustains proliferation of GCPs in culture (Dahmane and Ruiz-i-Altaba, 1999; Lewis et al., 2004; Wallace, 1999; Wechsler-Reya and Scott, 1999). Second, Shh expression at E17.5 to early postnatal stages is spatially restricted to the regions where fissures form first (Corrales et al., 2004; Lewis et al., 2004). Third, once the cells become postmitotic, the response of GCPs to Shh is greatly reduced (Corrales et al., 2004). Fourth, progressive deletion of *Shh* in mouse PCs using an *L7-Cre* transgene (Lewis et al., 2004) or inhibition of Shh by antibodies in the chick cerebellum (Dahmane and Ruiz-i-Altaba, 1999) results in reduced GCP proliferation and reduced foliation. Inactivation of mouse *Shh* during neural tube closure using *Pax2-Cre* results in a more severe phenotype (Lewis et al., 2004); however, we have recently shown an early requirement for *Shh* in setting up a normal cerebellar primordium (Blaess et al,

[1]Howard Hughes Medical Institute and Developmental Genetics Program, Skirball Institute of Biomolecular Medicine, [2]Department of Cell Biology, New York University School of Medicine, 540 First Avenue New York, NY 10016, USA. [3]Department of Physiology and Neuroscience, New York University School of Medicine, 540 First Avenue New York, NY 10016, USA.

*Present address: Howard Hughes Medical Institute and Department of Genetics, Boyer Center for Molecular Medicine, Yale University School of Medicine, New Haven, CT 06536, USA
†Author for correspondence (e-mail: joyner@saturn.med.nyu.edu)

Accepted 8 March 2006

2006). Thus, it remains unclear whether Shh is required after E16.5 for any fissures to form and whether Shh plays an instructive role in determining the pattern of folia.

All Shh signaling in patterning the mouse spinal cord is mediated by the three Gli transcription factors (Bai, 2004; Wijgerde et al., 2002). Genetic studies in the mouse have demonstrated that Gli3 functions primarily as a repressor, whereas Gli1 and Gli2 function as activators in the spinal cord (reviewed by Jacob and Briscoe, 2003). We have recently demonstrated that Gli2 is the major activator downstream of Shh in embryonic GCPs after E16.5 (Corrales et al., 2004). Although GCPs are specified normally in *Gli2*-null mutants, the external granule layer (EGL) is thinner and foliation is not initiated at E18.5. However, the lack of fissure formation could reflect either a delay in foliation because of reduced proliferation, or an absolute halt in foliation.

In a previous study, we identified a direct correlation between the spatial and temporal onset of fissure formation and elevated levels of Shh signaling in the developing cerebellum (Corrales et al., 2004). Here, we have tested the hypothesis that the level of Shh signaling determines the complexity of foliation in different mammals by analyzing mouse conditional mutants in which Shh signaling was progressively reduced or raised. Strikingly, we found that foliation proceeds in the absence of *Gli2*, but the progression of lobulation and growth of cerebellar lobules is delayed and prematurely halted. When *Gli1* is removed in addition to *Gli2*, foliation is further reduced. When all Shh signaling is removed after the cerebellar primordium is formed, all cerebellar foliation is inhibited because of a rapid depletion of GCPs after E17.5. Finally, raising Shh levels in PCs leads to formation of an additional fissure with a position conserved in rat. Thus, the level of Shh signaling regulates the extent of cerebellar foliation, but not the pattern.

MATERIALS AND METHODS

Generation of a targeting construct

A 3.0 kb *Not*I-*Spe*I genomic fragment of *Gli2* containing intron 6 was inserted into a targeting vector upstream of a *neo* cassette flanked with *Frt* sites, with one loxP site 3′ to the *neo* cassette and a *TK* cassette. Another loxP site containing an Asp718 site was inserted into a *Spe*I site within intron 9 in a 9.6 kb *Not*I-*Hin*dIII genomic fragment of *Gli2*. This fragment was then inserted 3′ to the loxP site contained in the original vector (Fig. 1A).

Breeding and genotyping of mice

One targeted W4 (Auerbach et al., 2000) ES cell clone was identified (Matise et al., 2000) from 122 G418 and GANC resistant cell clones by Southern blot analysis using Asp718 and a 3′ external probe from nucleotides 1290-2092 of the *Gli2* cDNA (encompassing exons 10-12) or using *Hin*dIII and an internal probe containing *neo* (see Fig. 1B). ES cell chimeras were generated through injection of C57BL/6 blastocysts (Skirball Transgenic Facility). Heterozygous $Gli2^{floxneo/+}$ offspring were bred with *ACTB-Flpe* mice (Rodriguez et al., 2000) to produce $Gli2^{flox/+}$ heterozygotes that were outbred to Swiss Webster mice.

We verified that recombination between the loxP sites produces a null allele by generating a deleted allele ($Gli2^{\Delta}$) and intercrossing them or breeding with mice carrying a null allele ($Gli2^{zfd/+}$) (Mo et al., 1997). Both $Gli2^{\Delta/\Delta}$ and $Gli2^{\Delta/zfd}$ E18.5 embryos displayed the same cerebellar phenotype described in $Gli2^{zfd/zfd}$ embryos (Corrales et al., 2004) (Fig. 1D-E; data not shown). Other phenotypes observed in $Gli2^{zfd/zfd}$ embryos (Matise et al., 1998; Mo et al., 1997; Palma and Ruiz i Altaba, 2004), such as lethality at birth, hydrocephaly, a curved body axis and abnormal patterning of the E10.5 ventral spinal cord were also present in $Gli2^{\Delta/\Delta}$ and $Gli2^{\Delta/zfd}$ mutants (C. B. Bai, unpublished; data not shown).

Double heterozygous mice ($En1^{Cre/+}$;$Gli2^{zfd/+}$) were crossed to Swiss Webster females to produce $En1^{Cre}$ $Gli2^{zfd}/En1^{+}$ $Gli2^{+}$ mice in which intrachromosomal recombination linked the $En1^{Cre}$ (Kimmel et al., 2000) and $Gli2^{zfd}$ (Mo et al., 1997) alleles. These mice were crossed to $Gli2^{flox/flox}$ mice to generate the conditional mutants $En1^{Cre}$ $Gli2^{zfd}/En1^{+}$ $Gli2^{flox}$ (*Gli2-En1* cko). $En1^{Cre}/Gli2^{zfd}$ mice which were also heterozygous for a null *lacZ* knock-in allele of *Gli1* (Bai et al., 2002), were bred with $Gli2^{flox/+}$ mice carrying the $Gli1^{lacZ}$ allele to generate $En1^{Cre}/Gli2$-cko;$Gli1^{lz/lz}$ mice. Other mutant alleles were genotyped as previously described: *Nestin-Cre* (Tronche et al., 1999), Smo^{flox} and Smo^{rec} (Long et al., 2001) and *Shh-P1* (Riccomagno et al., 2002). All mouse lines were maintained on an outbred Swiss Webster background. Although the cerebellar foliation pattern varies slightly between strains of mice (Inouye and Oda, 1980), in this outbred background we observed consistent foliation patterns in wild-type mice. The uvular sulcus (see Fig. 8 for definition), which is absent in some strains, was always present. The intraculminate fissure within lobule V, which varies in length between strains, was shallow in 80% of mice and the precentral a fissure that produces an additional tiny anterior lobule in FVBN mice was rarely present.

Noon of the day a vaginal plug was designated as E0.5. The day of birth was designated as P0. Adults were designated as P28 or older. For genotyping the $Gli2^{flox}$ allele, primers flanking the 3′ loxP site were used: floxC, 5′-AGGTCCTCTTATTGTCAGGC-3′; floxD, 5′-GAGACTCCA-AGGTACTTAGC-3′ (Fig. 1A). The mutant allele produced a 247 bp product, and the wild-type allele a 231 bp band (Fig. 1C). For detecting the recombined allele, $Gli2^{\Delta/+}$, primer sequences were 5′-CTTATGGA-CATCTGTCTGCC-3′ (floxA) and 5′-GAGACTCCAAGGTACTTAGC-3′ (floxD, see above). The recombined allele produces a 500 bp band (Fig. 1C).

Histology, immunocytochemistry and RNA in situ hybridization

For *lacZ* staining, brains were dissected fresh, embedded in OCT (Tissue-Tek) and sectioned at 20 μm. For histology and mice older than P8, either intracardiac perfusion was performed followed by immersion fix of tissue in paraformaldehyde (PFA) at 4°C, or freshly dissected brains were fixed overnight at 4°C using Carnoy. Tissue was then processed for paraffin embedding and sectioned at 7 μm. For consistency, sections analyzed from the vermis were limited to the most medial 100 μm. TUNEL assay was performed using ApopTag (Chemicon). Antibody staining was performed according to standard protocol. The following primary antibodies were used: rabbit α-BLBP (gift from N. Heintz), 1:3000; mouse α-calbindin (Sigma), 1:4000; rabbit α-cleaved caspase 3 (Cell Signaling), 1:2000; rabbit α-GFAP (Chemicon), 1:2000; mouse IgG α-NeuN (Chemicon), 1:2000. RNA in situ hybridization on sections was performed using standard methods. Detailed protocols are available at http://saturn.med.nyu.edu/research/dg/joynerlab

RESULTS

Generation of $Gli2^{flox}$ conditional mutant mice

In order to reduce Shh signaling and determine the requirement for positive Shh signaling through *Gli2* in cerebellar foliation, we generated mice carrying a conditional *Gli2* mutant allele, $Gli2^{flox}$ (Fig. 1A-C; see Materials and methods). Two loxP sites were inserted flanking exons 7 and 8, which are upstream of the exons encoding the zinc fingers. Deletion of these exons results in a frameshift mutation following splicing of mRNA from exon 6 to 9. The floxed allele was found to have wild-type activity, as $Gli2^{flox/flox}$ and $Gli2^{flox/zfd}$ mice appear normal (data not shown) and the deleted allele confers a null phenotype (Fig. 1D,E; see Materials and methods).

Deletion of *Gli2* in the midbrain and cerebellum after E9 rescues the lethal phenotype of *Gli2* null mutants

In order to generate a viable mutant in which *Gli2* was deleted from all cerebellar precursors, we used the $En1^{Cre/+}$ mouse line (Kimmel et al., 2000) in which *Cre* deletes target genes by E9.0 (Li et al., 2002) in all cells of the mesencephalon and rhombomere 1 (which gives rise to the cerebellum dorsally) (Zervas et al., 2004). *En1* and *Gli2* are separated by only 1.1 cM on chromosome 1; thus, mice in which $En1^{Cre}$ and $Gli2^{zfd}$ are linked were crossed to $Gli2^{flox/flox}$ mice to generate conditional mutants, referred to as *Gli2-En1* cko (conditional knockout) mutants (see Materials and methods).

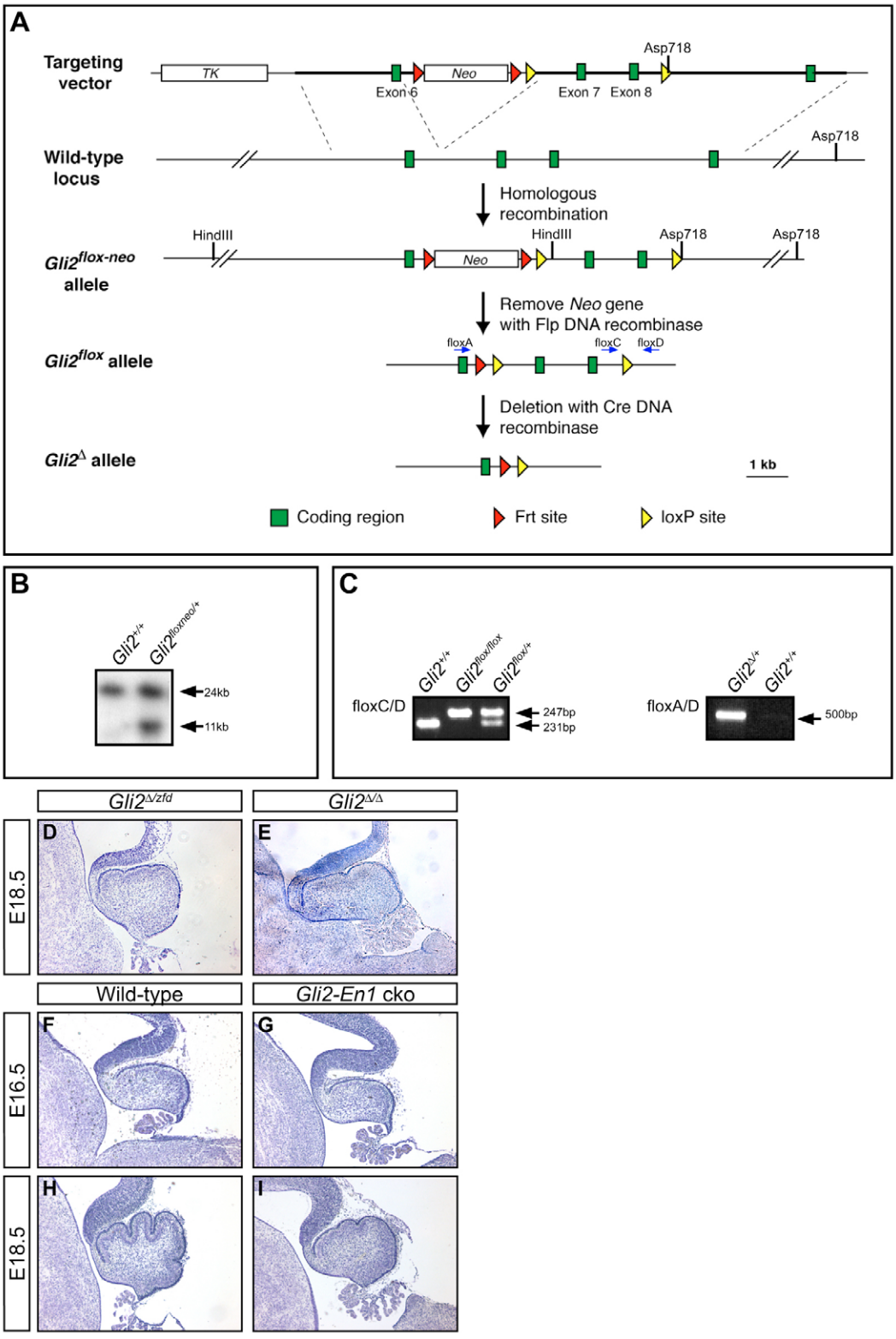

Fig. 1. Generation of a conditional allele and verifying the generation of a null allele. Schematic representation of the gene targeting strategy (**A**). A *neo* cassette flanked with *Frt* sites (red triangles) and two loxP sites (yellow triangles) were inserted into the *Gli2* locus using homologous recombination. ES cell clones were screened using Southern hybridization of Asp718-digested DNA with a 3′ external probe (**B**). PCR primers floxC and floxD flanking the 3′ loxP site (blue arrows, A) were used for genotyping (**C**). Primers floxA and floxD (blue arrows, A) were used to detect the recombined allele (C). The cerebella from $Gli2^{\Delta/zfd}$ (**D**) and $Gli2^{\Delta/\Delta}$ (**E**) embryos resembled the *Gli2*-null cerebellum, which lacks foliation. *Gli2-En1* cko mutants (**G**) at E16.5 appear similar in size and morphology to wild type (**F**). By E18.5, a reduction in foliation is observed in mutants (**I**) when compared with wild type (**H**).

We found that, indeed, *Gli2-En1* cko mutants were viable and the late embryonic cerebellar phenotype of *Gli2*-null mutant embryos was recapitulated. In sagittal sections, the E18.5 mutant cerebellum contained a thinner EGL and reduced foliation similar to *Gli2*-null mutants (Fig. 1H,I). Furthermore, wild-type and *Gli2-En1* cko cerebella appeared similar in volume and EGL thickness at E16.5 (Fig. 1F,G), supporting that the phenotype is due to the lack of response to Shh signaling from PCs around E18.5, rather than earlier expression of *Shh*. Importantly, *Gli2-En1* cko mice were detected at the expected Mendelian frequency of 50% at weaning. However, *Gli2-En1* cko adult mutants were only ~75% of the size of wild-type littermates and showed deficits in motor control consistent with cerebellar defects, including intention tremor, balance problems and a wide-based gait (data not shown).

Gli2 is required for the full extent of growth and elaboration of the cerebellar lobes, but not patterning

We next determined whether cerebellar foliation could occur after birth when positive Shh signaling is greatly reduced. Whole-mount analysis of *Gli2-En1* cko adult brains demonstrated an extreme decrease in the size of the cerebellum compared with wild type, whereas the rest of the brain appeared normal in size (Fig. 2A,D; data not shown). Of significance, fissures were observed in adult mutant cerebella, demonstrating that some foliation can occur in the absence of *Gli2*. The mediolateral extent of the adult mutant cerebellum appeared to be decreased less than the anteroposterior axis (arrows, Fig. 2A,D).

Horizontal and sagittal sections confirmed that the length of the *Gli2-En1* cko cerebellum along the mediolateral axis was not as drastically reduced compared with the anteroposterior axis and that the basic laminar structure was intact (Fig. 2C,F, shown schematically in Fig. 2C′,F′). Strikingly, the cardinal lobes were present in the mutant vermis and hemispheres, although the number of additional lobules was greatly reduced compared with wild type. In the vermis of *Gli2-En1* cko mutants, the fissure that normally divides the anterobasal lobe was absent or extremely shallow in six out of seven mutants, and the central lobe was divided by a shallow fissure in all mutants (arrows, Fig. 2B,E). In the hemispheres, the paramedial lobule was not subdivided in mutants and the fissures subdividing crus I and crus II were shallower in mutants than in wild types (Fig. 2C,F). Thus, the foliation pattern seen in *Gli2-En1* cko adults seems to reflect formation of only the earliest forming fissures, suggesting that foliation is initiated, but then does not progress to completion.

Progression of foliation is delayed and terminated prematurely in *Gli2-En1* cko mutants

We next determined whether the sequential generation of folia progressed normally but did not reach completion in *Gli2-En1* cko mutant cerebella. Although P0 wild-type and mutant cerebella appeared similar in whole mount (Fig. 3A,B), by P2, *Gli2-En1* cko mutant cerebella were obviously smaller than normal along the AP axis (Fig. 3E,F), and by P5 the difference was striking (Fig. 3I,J). In wild-type brains, the cerebellum continues to grow until P16, whereas in the *Gli2-En1* cko mutants, the cerebellum did not appear to increase in size after P8 (Fig. 3M,N,Q,R).

Analysis of sagittal sections delineated the manner by which the adult foliation pattern arose. On the day of birth, a mutant phenotype was clearly visible in sagittal sections. In wild-type cerebella, the four principle fissures had begun to form and the anterobasal lobe was beginning to be further divided (Fig. 3C). In the mutant, only slight indentations corresponding to the preculminate, primary and posterolateral fissures that produce the cardinal lobes were discernable (Fig. 3D). At P2 in the wild type, the central lobe had begun to be divided by one fissure, whereas in the *Gli2-En1* cko mutant only four fissures were present, reminiscent of the principle fissures seen in wild-type E18.5 cerebella (Fig. 3G,H compare with 3C). By P5 in the wild-type cerebellum, all lobules had formed and two sublobules had begun to form (Fig. 3K). By contrast, the mutant contained only the four principle fissures and a shallow prepyramidal fissure in the central cardinal lobe (Fig. 3L). The wild-type cerebellum continued to grow extensively until P16 and all lobulation and sublobulation was initiated by P8 (Fig. 3O). The *Gli2-En1* cko mutant cerebellum, by contrast, grew little between P5 and P8 and then stopped growing. Furthermore, foliation had only progressed to include a very slight division of the anterobasal lobe in mutants at P8 (asterisk, Fig. 3P). The adult (P28) *Gli2-En1* cko mutant cerebellum was similar in size to the P8 mutant cerebellum and did not develop additional fissures, although the mutant IGL was more compact at P16 than at P8 (Fig. 3S,T). The final foliation pattern of the *Gli2-En1* cko cerebellum was therefore similar to that of a P2 wild-type cerebellum.

The EGL is depleted earlier than normal in *Gli2-En1* cko mutants

We next determined the cellular basis of the decreased foliation and growth in *Gli2-En1* cko cerebella. As *Gli2*-null mutants have a thinner EGL at E18.5 (Corrales et al., 2004) and GCP proliferation is required for foliation, we examined the EGL in postnatal *Gli2-En1* cko mutants. At birth, the wild-type EGL is thicker at the base of

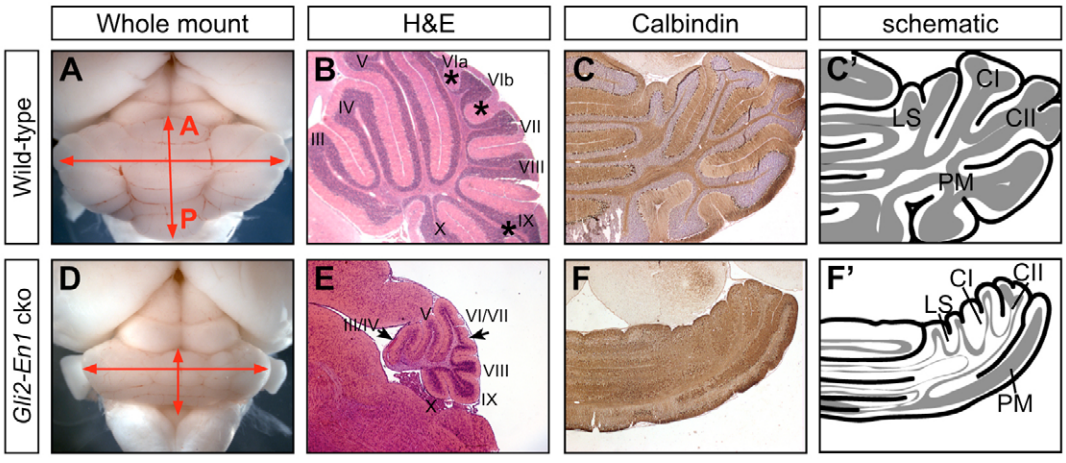

Fig. 2. Whole-mount and histological analysis shows decreased complexity of foliation in adult *Gli2-En1* cko mutants. Cerebellar size is severely compromised along the anteroposterior (AP) axis in mutants, but the mediolateral extent is similar to wild type (**A**,**D**). Sagittal sections show fewer fissures in the vermis of the mutant (**B**,**E**). Some fissures in the mutant are barely detectable (arrows, E) and others are completely absent (asterisks, B). Horizontal sections highlight the similar mediolateral size of wild types and mutants; the mutant cerebellum is reduced in size along the AP axis (**C**,**F**, shown schematically in **C**′,**F**′). The fissures in the mutant are much shallower than in wild type. Abbreviations: LS, lobulus simplex; CI, crus I; CII, crus II; PM, paramedial lobule.

each fissure and overall is thinnest in the central region; however, this variation is minimal at later stages. We found that in the wild type, the EGL varied from two to four cells; however, the EGL in mutants was only one or two layers thick (Fig. 3U,X). In addition, the difference in thickness was more drastic at the base of the fissures than at the crowns of the lobes. At P5, the *Gli2-En1* cko mutant EGL contained one to four layers, rather than the eight to ten layers present in the wild type (Fig. 3V,Y). Strikingly, whereas the eight to ten cell layers of GCPs persisted in the wild-type EGL to P8, the mutant EGL was completely depleted of cells by P8 (Fig. 3W,Z). In wild-type mice, the EGL persisted and the cerebellum continued to grow until P16. In summary, the reduced thickness of the EGL in *Gli2-En1* cko mice as early as E18.5 correlates with a delay in onset of foliation. Furthermore, the delay and a premature depletion of the EGL correlate with a reduction in the complexity of foliation.

Laminar organization is grossly normal in *Gli2-En1* cko mutants

It was important to determine whether the foliation defect in *Gli2-En1* cko cerebella was due simply to a defect in the response of GCPs to Shh, or whether other cell types were also abnormal. Based on expression of the Hh target gene *Gli1*, the response to Shh

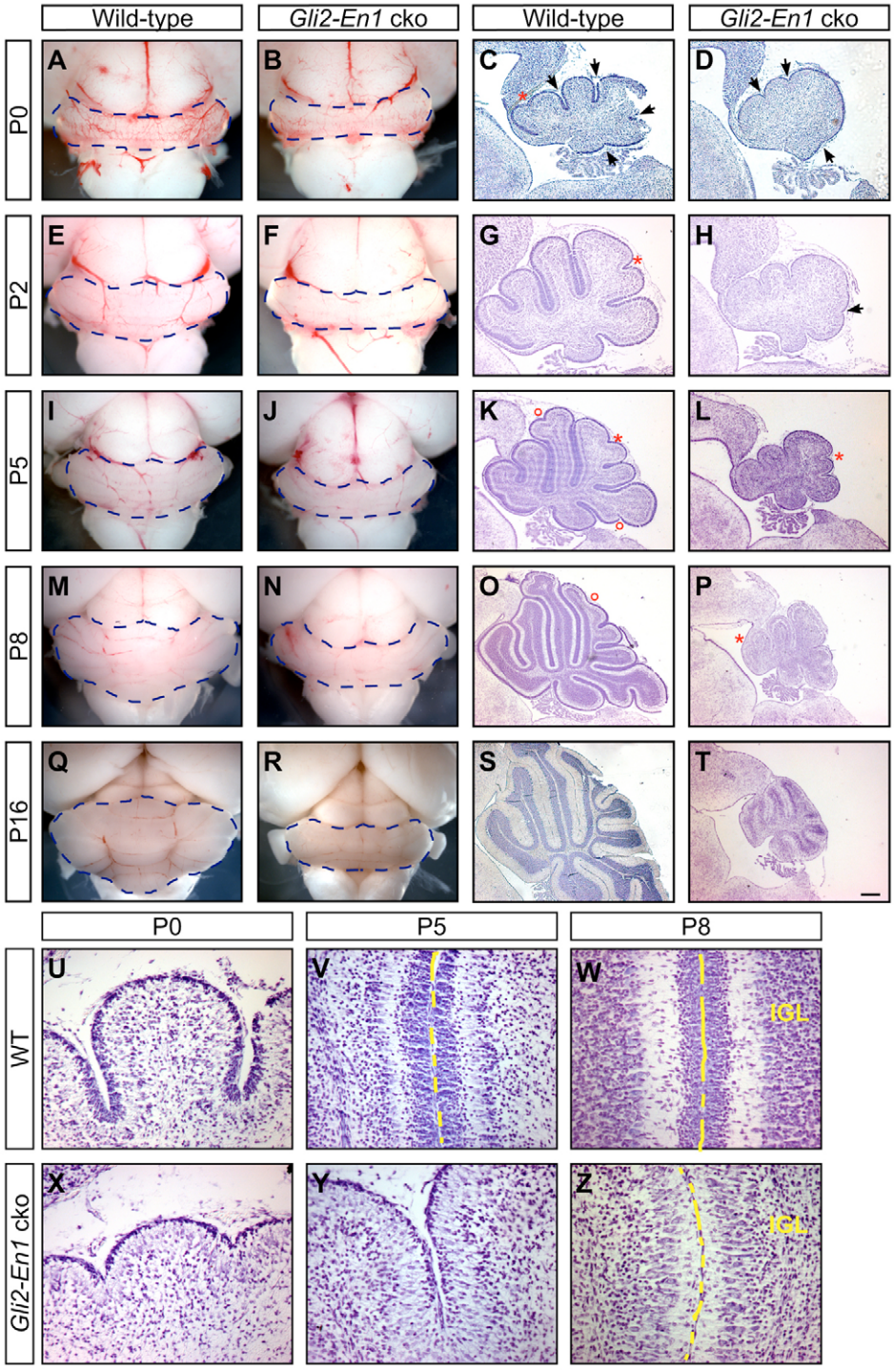

Fig. 3. Developmental series analysis reveals a delay and premature termination of foliation. At P0, the wild-type (**A**) and *Gli2-En1* cko mutant (**B**) cerebella appear similar in size in whole mount. By P2, a slight difference in size is observed between wild type (**E**) and mutant (**F**). The mutant cerebellum at P5 (**J**) is clearly smaller than that of the wild-type (**I**). Histological analysis of sagittal sections at P0, P2, and P5 of wild-type (**C**,**G**,**K**) and *Gli2-En1* cko (**D**,**H**,**L**) cerebella show shallower fissures, and a thinner EGL in mutants. (**M-T**) The mutant cerebellum does not increase in size after P8 (N,P,R,T) compared with the continued growth observed after P8 in wild-type (M,O,Q,S). The overall anteroposterior pattern of foliation appears intact, although the number of fissures present in P16 mutants (T) is comparable to the number present in wild type at P2 (S). (**U-Z**) At P0, the mutant EGL (X) is thinner than in wild type (U). By P5, the wild-type EGL has thickened to more than 10 cell layers (V), whereas the mutant EGL contains 2-4 cell layers (Y). By P8, the wild-type EGL remains thick (W), in contrast to the mutant EGL, which has been depleted (Z). Arrows indicate principle fissures forming cardinal lobes, asterisks indicate fissures forming lobules and open circles represent fissures forming sublobules. Broken yellow line indicates pial surface between two lobules; broken blue line outlines the cerebellum. Scale bar: 250 μm in C,D,G,H; 350 μm in K,L; 500 μm in O,P,S,T.

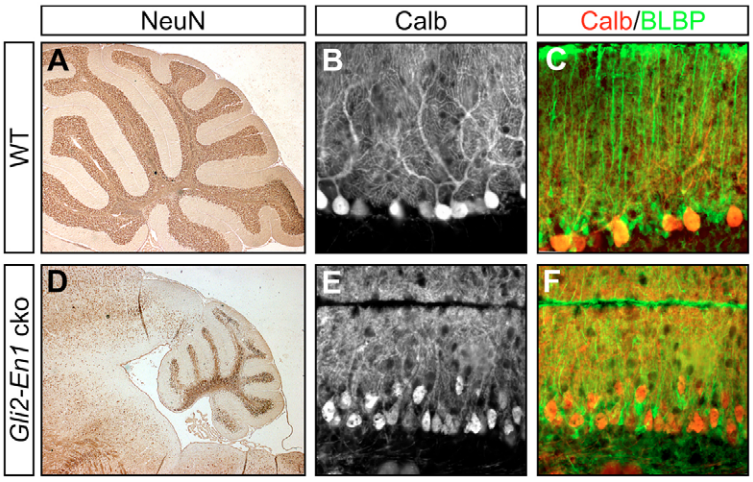

Fig. 4. Laminar organization is grossly normal in *Gli2-En1* cko cerebella. The internal granule layer (IGL) containing differentiated granule cells marked by NeuN is extremely sparse in mutants (**D**) compared with wild type (**A**). The PCs, marked by calbindin, are multilayered with less elaborate dendritic arborization in mutants (**E**), in contrast to the monolayer and complex arborization in wild type (**B**). The Bergmann glia marked by BLBP in green, are interspersed with the PCs (red); however, the glial fibers appear disorganized in mutants (**F**) compared with wild types (**C**).

signaling is highest in proliferating GCPs and Bergmann glia, and absent in PCs (Corrales et al., 2004). A reduction in positive Shh signaling could therefore directly alter formation of the IGL and/or differentiation of Bergmann glia. The spreading out of PCs into a monolayer could also be indirectly affected because of the reduced surface area.

Indeed, the IGL (as visualized by immunohistochemistry for NeuN) in adult mutants was significantly thinner compared with wild type and the GCs formed a less compact IGL (Fig. 4A,D). Consistent with the decrease in the surface area of the cerebellum, the PCs (visualized with calbindin immunostaining) remained multilayered in *Gli2-En1* cko mutants, instead of forming a monolayer as observed in wild types (Fig. 4B,E). In addition, the dendritic arborization of the PCs in the molecular layer of mutants was less branched than normal. As each PC dendrite normally contacts tens of thousands of parallel fibers of GCs in the molecular layer (Ito, 1984), and contact with GCs drives PC differentiation (Baptista et al., 1994), the reduction of GCs in *Gli2-En1* cko mutants is expected to cause a decrease in the complexity of the mutant PC dendrites. The reduced number of GCs in *Gli2-En1* cko mutants did not, however, appear to lead to PC degeneration as calbindin staining in 6-month-old brains was similar to that observed in mutants at P28 (data not shown).

A previous in vitro study suggested a role for Shh in differentiation of the Bergmann glia (Dahmane and Ruiz-i-Altaba, 1999). To determine whether Bergmann glia were altered in *Gli2-En1* cko mutants, we used antibody labeling for the Bergmann glial markers BLBP and GFAP. Cells positive for both antibodies were present in *Gli2-En1* cko mutants, demonstrating that Shh signaling through Gli2 is not required for Bergmann glial specification (Fig. 4C,F; data not shown). However, Bergmann glia were morphologically abnormal. Although the soma of Bergmann glia were interspersed among the PCs in *Gli2-En1* cko mutants, their glial fibers were misshapen and disorganized compared with the ordered and linear morphology of wild-type Bergmann glial fibers (Fig. 4C,F). This phenotype could reflect either a direct role for Shh signaling through Gli2 in Bergmann glial maturation, or a secondary defect resulting from disorganization of the PC layer and reduction in GCs.

Removing the Gli1 activator further reduces foliation in *Gli2-En1* cko cerebella

We have previously shown that in the cerebellum of E18.5 *Gli2* null mutants, expression of *Gli1* is drastically reduced but not absent and *Gli1* mutants have a normal cerebellum (Corrales et al., 2004). To determine whether Gli1 contributes activator function in *Gli2-En1* cko mutants that is responsible for the low level of GCP proliferation and foliation present in *Gli2-En1* cko mutants, we generated *Gli2-En1* cko mice with reduced or no *Gli1*. We analyzed eight litters from a cross between $En1^{Cre}$ $Gli2^{zfd}/En1^{+}$ $Gli2^{+}$;$Gli1^{lz/+}$ and $Gli2^{flox/f+}$;$Gli1^{lz/+}$ mice, but only one *Gli2-En1* cko;$Gli1^{lz/lz}$ mouse survived, as $Gli2^{+/-}$;$Gli1^{-/-}$ mice have an extremely low survival rate (Park et al., 2000). *Gli2-En1* cko;$Gli1^{lz/+}$ mice, however, were generated with the expected frequency. Although *Gli2-En* cko;$Gli1^{lz/+}$ mice had the same phenotype as *Gli2-En1* cko mice (data not shown), the *Gli2-En1* cko;$Gli1^{lz/lz}$ mutant cerebellum had a decreased number of fissures compared with *Gli2-En1* cko mutants (Fig. 5B,C compare with Fig. 3T). In medial sections of the cerebellum, only the five cardinal lobes could be discerned. The decreased number of lobules that formed in the *Gli2-En1* cko;$Gli1^{lz/lz}$ mutant shows that Gli1 does indeed contribute to foliation in *Gli2-En1* cko mutants.

Shh signaling is required for cerebellar foliation

Our finding that removing both *Gli1* and *Gli2* activators did not inhibit formation of the cardinal lobes raised the issue of whether Shh is required at all for the initial simple foliation pattern seen in all mammals. Although conditional removal of Shh using *Pax2-Cre* and *L7-Cre* did not fully inhibit foliation, the degree of recombination in these mutants is not clear (Lewis et al., 2004). We therefore analyzed cerebellar development in the absence of *Smo*, by generating viable conditional mutants for *Smo* in the brain using a floxed *Smo* allele (Long et al., 2001). As the cerebellar primordium is compromised in $En1^{Cre/+}$;$Smo^{flox/-}$ (*Smo-En1* cko) mutants by E12.5 and the mutants die at birth (Blaess et al., 2006), we used *Nestin-Cre* transgenic mice (Graus-Porta et al., 2001; Tronche et al., 1999) to delete *Smo* throughout the CNS, and in rhombomere 1 beginning around E11 (Blaess et al, 2006). Approximately 10% of *Nestin-Cre;Smo*-cko (*Smo-Nes* cko) mutants survive to three weeks [data not shown; see Machold (Machold, 2003)]. The cerebellar primordium of these mutants is grossly normal at E16.5, although slightly reduced in size (Blaess et al., 2006). The overall size of the P21 *Smo-Nes* cko mutant brains was smaller than wild type, although the cerebella showed a more pronounced reduction in size. As in the *Gli2*-cko mutants, the AP axis of the cerebellum was more dramatically reduced than the ML axis. Interestingly, histological analysis of midsagittal sections of P16-21 *Smo-Nes* cko brains showed a foliated cerebellum that consisted of five cardinal lobes in all but one mutant (n=4), although the four principle fissures were very shallow (Fig. 5D). In one mutant, extremely shallow fissures

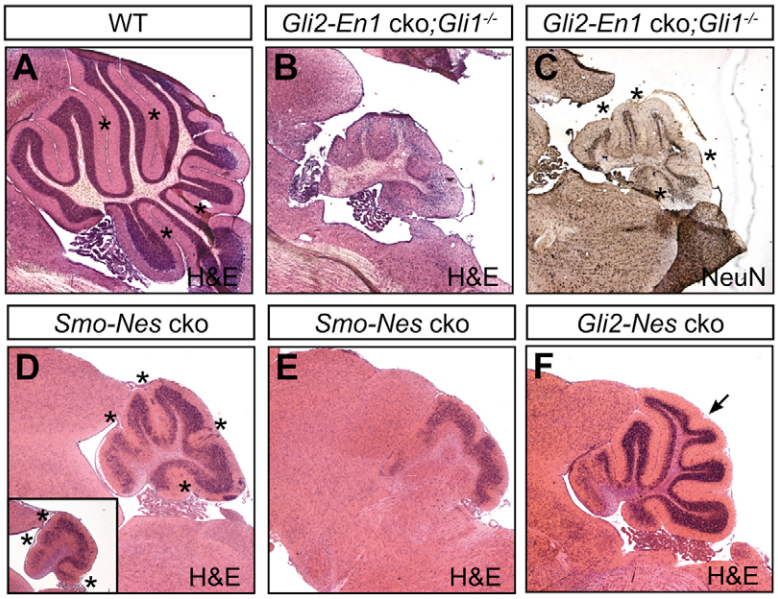

Fig. 5. Removal of Gli activator further reduces foliation in *Gli2-En1* cko cerebella. Histological analysis of sagittal sections reveal that only principle fissures form in the absence of *Gli1* and *Gli2* (**A**,**B**). Marking differentiated neurons with NeuN shows few GCs and a thin IGL in *Gli2-En1* cko;*Gli1*$^{-/-}$ mutants (**C**). In *Smo-Nes* cko mutants, only the principle fissures form in medial sections (**D**) and little foliation occurs in lateral sections (**E**). This phenotype varies (D, inset). *Gli2-Nes* cko mutants develop more fissures (arrow, **F**) than *Gli2-En1* cko mutants (see Fig. 4). Scale bar: 500 μm.

were observed corresponding to the positions of three of the four principle fissures (Fig. 5D, inset). Furthermore, the depth of the fissures in the medial vermis varied between animals. However, a basic layered cytoarchitecture with an IGL was present. By contrast, in some regions of lateral sections of P21 *Smo-Nes* cko cerebella foliation was limited to slight indentations only in the central and posterior regions (Fig. 5E).

One possible reason for a more severe phenotype in the lateral cerebellum, and the different degrees of phenotypes in the vermis, is inefficient recombination of the *Smo* conditional mutant allele in the vermis compared with the hemispheres, and to varying degrees in different animals. To determine whether this was the case, expression of *Gli1* was analyzed in E18.5 *Smo-Nes* cko mutants as a readout of residual Shh signaling. Indeed, patchy *Gli1* expression was detected in the EGL of E18.5 *Smo-Nes* cko brains, primarily in medial sections (see Fig. S1A in the supplementary material), although no expression was observed in the Bergmann glial layer where *Gli1* is normally expressed. Furthermore, in lateral sections, *Gli1* expression was only detected in regions that give rise to the central and posterior lobes (Fig. 6A). Thus, *Gli1* expression correlates with areas of foliation, indicating that foliation only occurs if wild-type GCPs are induced to proliferate in response to Shh signaling. The correlation between the loss of *Gli1* expression in regions of the lateral EGL of E18.5 *Smo-Nes* cko mice and lack of fissures demonstrates that Shh signaling is absolutely required after birth for cerebellar foliation. *Math1*-positive proliferating cells were observed throughout the EGL of E18.5 *Smo-Nes* cko and *Smo-En1* cko embryos (Fig. 6B and data not shown), demonstrating that GCPs are generated independent of Shh signaling, but require Shh for continued proliferation in the EGL after birth.

The foliation present in *Gli2-En1* cko mutants was not due to inefficient recombination of *Gli2*^{flox}, as *Gli1* was not detected in P2 medial or lateral cerebellar sections in these mutants (see Fig. S1C,D in the supplementary material; data not shown). We analyzed the cerebellum phenotype of *Nestin-Cre;Gli2*$^{flox/-}$ (*Gli2-Nes* cko) mice as the mosaicism found using *Nestin-Cre* was expected to allow foliation to progress further than in *Gli2-En1* cko mutants. Indeed, compared with *Gli2-En1* cko mutants, the *Gli2-Nes* cko vermis contained a more defined intercrural fissure (arrow, Fig. 5F) and a thicker IGL than in *Gli2-En1* cko mice. Recombination in these mutants was also mosaic, as demonstrated by patchy expression of *Gli1* in *Gli2-Nes* cko mutants at P0 (see Fig. S1E,F in the supplementary material).

Shh is not absolutely required for *Mycn* and cyclin D1 expression

The proto-oncogene *Mycn* (previously *Nmyc*) is a potential downstream effector of GCP proliferation via Shh signaling, as it regulates proliferation and is a direct target of Shh in GCPs (Kenney et al., 2003). Mycn probably mediates GCP proliferation via cyclin D1, as cyclin D1 mRNA (*Ccnd1*) is also upregulated in response to Shh in GCPs (Kenney and Rowitch, 2000). We therefore examined the expression of *Mycn* and *Ccnd1* in the absence of *Gli2* in the cerebellum. In the wild-type cerebellum at P0, *Mycn* and *Ccnd1* expression was observed in the EGL along the anteroposterior axis and some *Ccnd1* expression was also detected in a deeper layer, which could correspond to the Bergmann glial layer (Fig. 6C,D). This expression pattern differs from that of *Shh* and *Gli1*, which are higher in the anterior cerebellum during early postnatal stages (Corrales et al., 2004). At P0, expression of both *Mycn* and *Ccnd1* was reduced in the EGL of *Gli2-En1* cko mutants, although expression of both genes was not abolished (Fig. 6E,F). It is likely that the reduction in expression is due in part to the decreased number of GCPs in the EGL, in addition to a direct effect of decreased Shh signaling.

One possibility was that the remaining *Mycn* and *Ccnd1* expression was due to activator function of Gli1 or Gli3. We tested this by analyzing *Smo-Nes* cko mutants. In lateral sections of E18.5 *Smo-Nes* cko mutants, where recombination was complete, based on *Gli1* expression (compare Fig. 6A and Fig. S1A in the supplementary material), both *Mycn* and *Ccnd1* were downregulated, although some expression of both genes persisted (Fig. 6G,H). Thus, although Shh signaling through Gli activators is not absolutely required for the expression of *Mycn* and *Ccnd1*, it upregulates their expression.

Increased Shh signaling produces a more complex foliation pattern

Based on our finding that a reduction in Shh signaling results in less foliation with a corresponding reduction in the temporal length of GCP proliferation, we addressed whether increasing Shh could

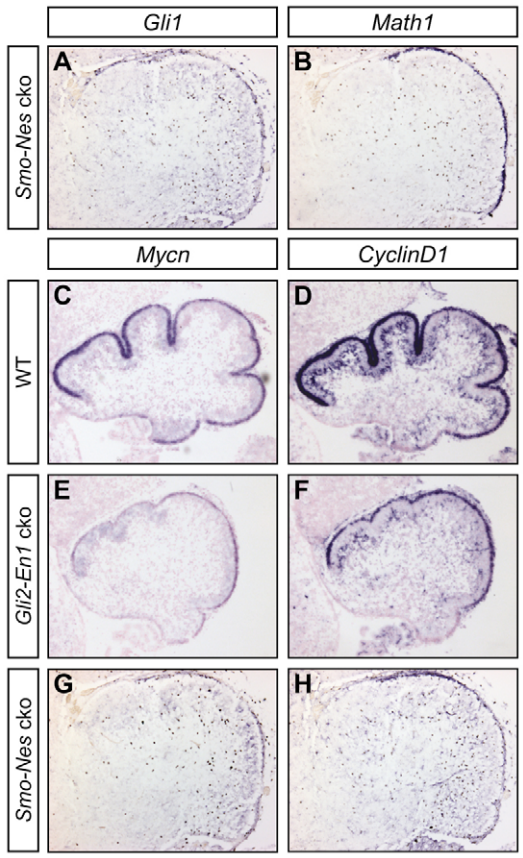

Fig. 6. Cell cycle genes *Mycn* and cyclin D1 (*Ccnd1*) are downregulated in *Smo-Nes* cko and *Gli2-En1* cko cerebella. RNA in situ hybridization shows downregulation of the transcriptional target of Shh, *Gli1*, in *Smo-Nes* cko mutants at E18.5 (**A**), although expression of *Math1* (**B**) indicates the presence of GCPs. Another transcriptional target of Shh, *Mycn*, is downregulated in *Smo-Nes* cko at E18.5 and *Gli2-En1* cko mutants at P0, respectively (**E**,**G**), compared with wild types (**C**). *Ccnd1*, which is downstream of *Mycn*, is also downregulated but still present in mutants (**F**,**H**) compared with wild types (**D**).

induce additional foliation We previously have shown that *Shh-P1* transgenic mice (*Shh-P1*) (Riccomagno et al., 2002) have increased levels of Shh signaling and GCP proliferation extends for an additional 2 days (Corrales et al., 2004). Furthermore, these mutants develop a larger cerebellum with a thicker and irregular IGL. Upon more extensive examination of many mutants, we discovered that bulges in the IGL of *Shh-P1* cerebella were consistently found in specific positions (Fig. 7B). This suggested that an underlying genetic mechanism controls where bulges form when the number of GCPs is increased. To test whether further increasing Shh signaling can lead to formation of fissures in defined positions, we generated *Shh-P1* mice which were heterozygous for a mutation in patched (*Ptch1*), a receptor for Shh which functions to inhibit Shh signaling (Goodrich et al., 1997). Consistent with our prediction, *Shh-P1;Ptch1*$^{+/-}$ mice not only had larger cerebella than *Shh-P1* mice, but also had an extra sublobule on the rostral face of lobule VI (*n*=3/4) (arrow, Fig. 7C). Interestingly, the position of this sublobule is reminiscent of sublobule VI-d in the rat cerebellum (arrow, Fig. 7D). In combination with the decreased fissure formation in *Gli2*-cko and *Smo*-cko mutants, these results demonstrate a direct link between the level of Shh signaling and complexity of the cerebellar foliation pattern via regulation of GCP proliferation. The *Shh-P1* transgene did not, however, enhance foliation in *Gli2-En1* cko cerebella (see Fig. S2B,C in the supplementary material), demonstrating that the remaining Gli proteins are not sufficient to drive additional GCP proliferation.

DISCUSSION

The level of Shh signaling regulates the extent of elaboration of mouse cerebellar lobules

Using conditional mutagenesis, we have generated an allelic series of mutant mice with varying levels of Shh signaling in the cerebellum (summarized in Fig. 8). Complete removal of the transmembrane receptor Smo abolishes Shh signaling through Gli activators and the Gli3 repressor is upregulated. As a result, we found that GCPs proliferate only until soon after birth and no foliation occurs. However, when Shh signaling is reduced by removing *Smo* in a mosaic fashion or by removing all *Gli1* and *Gli2*, only the fissures that produce the cardinal lobes form. Foliation in *Gli2-En1* cko mutant cerebella progresses a little further with formation of two additional shallow fissures and longer lobules. Mosaic removal of *Gli2* allows slightly more foliation. Complementary to this, in *Shh-P1;Ptch1*$^{+/-}$ mice that have increased levels of Shh signaling in the cerebellum, an additional fissure forms in a position corresponding to sublobule VI-d in the more elaborately foliated rat cerebellum. Thus, the extent of foliation in these mutants correlates with the level of Shh signaling and the pattern of the fissures corresponds to normal developmental progression of foliation.

Despite there being a simpler foliation pattern in the *Smo* cko and *Gli2* cko mutants, the patterns seen along the anteroposterior and mediolateral axes represent the conserved pattern seen in all

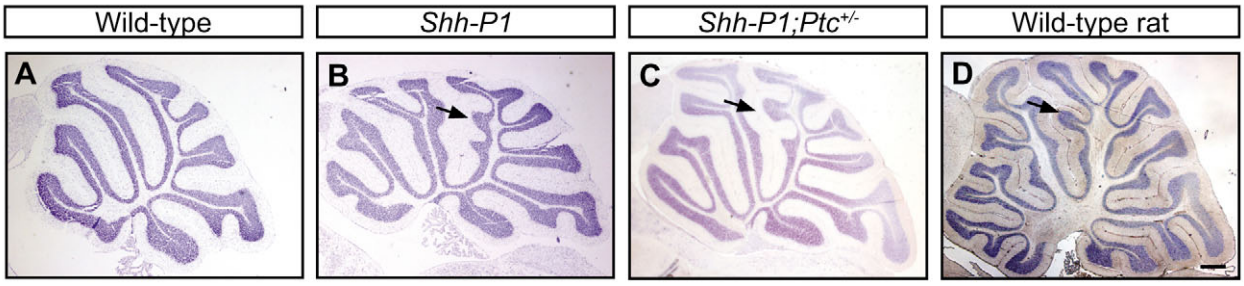

Fig. 7. The level of Shh signaling correlates with size and number of lobules. Histological analysis of adult cerebella shows *Shh-P1* transgenics (**B**) have a larger cerebellum than normal (**A**), with longer lobules and bumps in specific locations (e.g. arrow). *Shh-P1;Ptch1*$^{+/-}$ mutants (**C**) also have longer lobules and an extra sublobule forms (arrow) which corresponds to a sublobule (arrow) present in the adult rat (**D**). Scale bar: 500 μm.

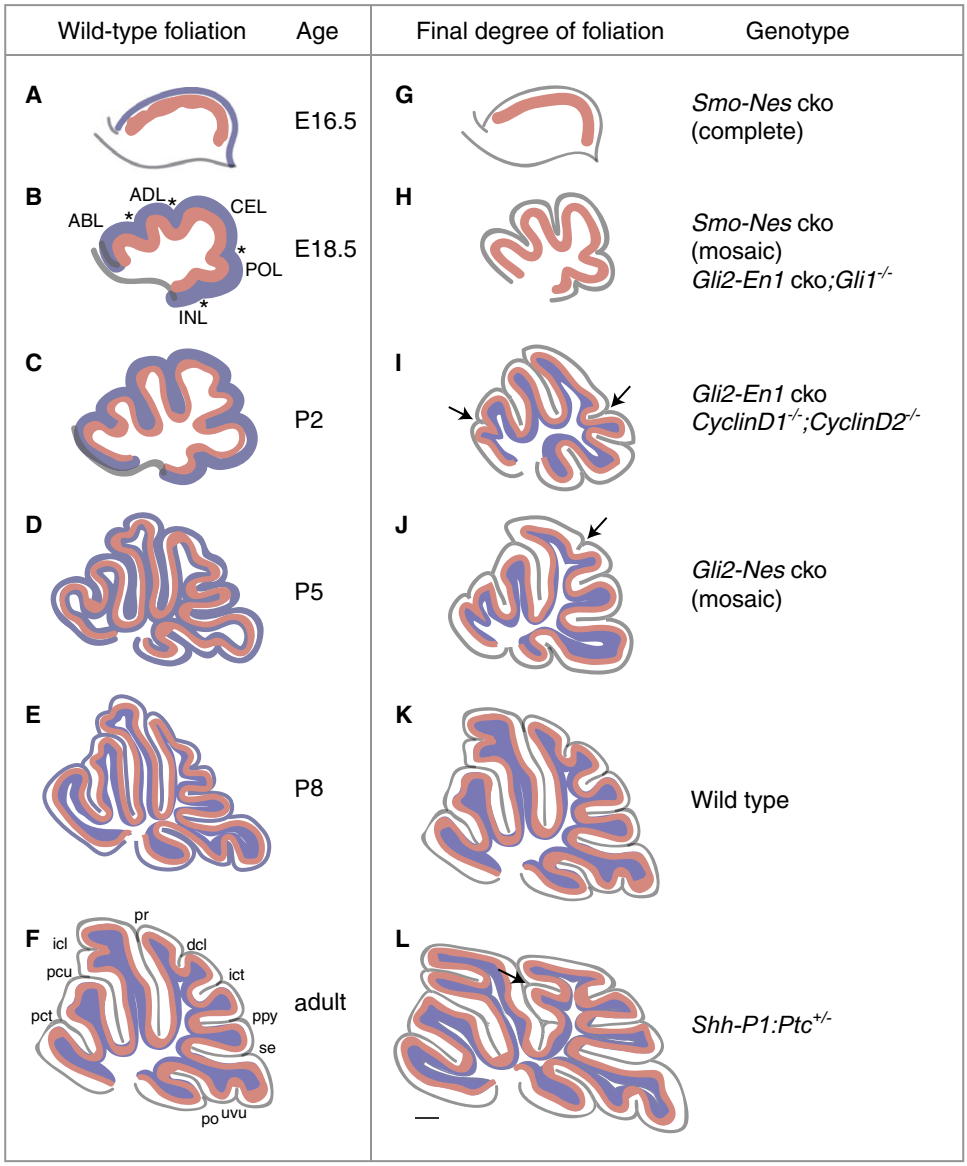

Fig. 8. A graded series of Shh signaling levels generates varying degrees of fissure formation in the cerebellum. (**A-L**) Schematics of sagittal sections show the morphology of normal cerebella at different stages as well as adult mutants. (B) Principle fissures at E18.5 are marked with asterisks. (G) In the absence of Smo function, no fissures form. (H) Mosaic removal of *Smo* allows partial rescue by the remaining wild-type cells, and the principle fissures form, similar to the pattern present in E18.5 wild-type cerebella. A similar pattern of fissures forms when only *Gli3* is present. (I) In the absence of *Gli2*, lobulation progresses slightly further, such that two additional fissures form (arrows), as in P2 wild-type cerebella. (J) Mosaic removal of *Gli2* allows an additional fissure to form (arrow). (L) When excess Shh signaling occurs, lobulation progresses further than normal. Pink indicates the PC layer, and blue represents GCPs and GCs. Abbreviations: ABL, anterobasal lobe; ADL, anterodorsal lobe; CEL, central lobe; POL, posterior lobe; INL, inferior lobe; pct, precentral; pcu, preculminate; icl, intraculminate; pr, primary; dcl, declival; intercrural, itc; ppy, prepyramidal; se, secondary; uvu, uvular; po, posterolateral). Figures not drawn to scale. Scale bar: 400 μm in A-C,G-J; 425 μm in D,D; 500 μm in F,K-L.

mammals. This result suggests that Shh signaling does not determine the position of the fissures, or the differential patterning of the vermis and hemispheres. Shh is instead a permissive factor for foliation. Our discovery supports a previously proposed model that positioning of the fissures is determined by interactions between PCs and mossy fibers as well as GC parallel fibers (Altman and Bayer, 1997). Another theory for the mechanism of foliation is that differential rates of proliferation in the EGL (with a greater rate in the depths of the fissures) causes buckling forces to generate fissures (Mares and Lodin, 1970). Although we cannot exclude this model, as Shh signaling is even along the base and the crown of the lobules (Corrales et al., 2004), Shh does not appear to influence the complexity of foliation by regulating the rate of proliferation.

Taken together, the *Gli2* cko and *Smo* cko results support a conserved multiphasic process of foliation similar to that proposed for rat by Altman and Bayer (Altman and Bayer, 1997). Initially, the smooth cerebellar primordium is divided by the four principle fissures to generate the five cardinal lobes (indicated in Fig. 8). These are then divided into lobules, and some are subsequently divided into sublobules. The selective elimination of GCPs at late embryonic or early postnatal stages in rat (Doughty et al., 1998) or hyperthyroidism in mice, which causes premature depletion of the EGL (Lauder et al., 1979), produce less complex foliation patterns similar to the allelic series we created by selectively eliminating components of the Shh signaling pathway. In accordance with Shh being expressed by Purkinje cells and the necessary interaction between PCs and GCs for foliation, many mutant mice with defects in PC development have a decrease in foliation. For example, in *staggerer* and *lurcher* mutants, foliation occurs to a similar degree as in our two *Gli2* cko mutants and have phenotypes similar to those depicted in Fig. 8H,J, respectively (Caddy and Biscoe, 1979; Herrup, 1983; Sidman et al., 1962; Wetts and Herrup, 1982). Conversely, the foliation process is prolonged and the number of fissures is increased in cases of hypothyroidism, which prolongs the presence of the EGL (Lauder et al., 1979), similar to transgenic mice with increased Shh signaling.

Our results show that only a very minimal level of Shh signaling is required for the initial phase of cardinal lobe formation, whereas a higher level and sustained signaling is necessary for partitioning of the cardinal lobes into lobules and sublobules. Furthermore, the

cerebellar phenotype of *Gli2-En1* cko mice demonstrates that Shh signaling through Gli2 is not required for generation of the cardinal lobes, but instead is required to maintain the proliferative pool of GCPs such that a sufficient number of GCs are generated to achieve full lobe growth, and to complete the lobulation and sublobulation processes.

Gli2 is not required for cell type specification in the cerebellum

It was previously unknown whether Shh signaling through Gli2 regulates cell type-specific differentiation in the cerebellum. In the spinal cord, Shh signaling through Gli2 is required for the induction of the two most ventral cell types (Matise et al., 1998; Mo et al., 1997), and both Gli2 and Gli3 influence the normal differentiation of the other ventral cell types (Bai, 2004; Stamataki et al., 2005). A high level of positive Shh signaling is restricted to the proliferating GCPs and Bergmann glia (based on *Gli1* expression) and thus could influence their differentiation (Corrales et al., 2004). We found that in *Gli2-En1* cko mutants both of these cell types are in fact generated, although the GC population is reduced in number. The depletion of GCPs in *Gli2* cko mutants probably causes a less compact IGL to form and the lack of spreading out of the PCs into a monolayer. Furthermore, the decreased number of differentiated GCs could account for the abnormal PC dendrite morphology in *Gli2* cko mutants. Thus, the defects in GCs and PCs are probably not due to direct effects on differentiation of either cell type.

Although Bergmann glia form in *Gli2* cko mutants, their fibers are disorganized. As Bergmann glial fibers are known to enwrap synapses on PC dendrites (Yamada et al., 2000), the Bergmann glial phenotype could be secondary to the observed abnormal PC morphology. Conversely, Bergmann glial fibers are thought to shape the dendritic morphology of PCs (Lordkipanidze and Dunaevsky, 2005); therefore, abnormal glial development may cause secondary effects on PC development. Consistent with this, *Gli1* and *Gli2* are both expressed in Bergmann glia (Corrales et al., 2004), and thus Shh signaling could have a direct effect on the final steps of Bergmann glia differentiation. The expression of the late marker GFAP in mutants shows that Bergmann glia differentiation nevertheless proceeds quite far. Furthermore, although disorganized, the glial fibers extend to the pial surface of the cerebellum as in wild-type mice. Finally, the Bergmann glia in *Gli2* cko mutants appear similar to those in agranular rat cerebella (Doughty et al., 1998). A cell type specific conditional knock-out of *Gli2* in Bergmann glia is needed to resolve which cellular defects are primary versus secondary.

Shh is not absolutely required for *Mycn* and *Ccnd1* expression

Shh signaling has been found to regulate proliferation in the skin and hair by inducing cell cycle genes (Fan and Khavari, 1999; Mill et al., 2003; Mill et al., 2005) and both *Mycn* and *Ccnd1* are upregulated by Shh signaling in GCPs (Kenney et al., 2003; Oliver et al., 2003). Interestingly, mice mutant for both *Ccnd1* and *Ccnd2* have a small cerebellum (Ciemerych et al., 2002), with a foliation pattern similar to that observed in *Gli2-En1* cko mutants. We unexpectedly found that although *Mycn* and *Ccnd1* are reduced in the absence of either *Smo* at E18.5 or *Gli2* at P0, expression is not abolished. In addition, *Mycn* expression levels do not correlate spatially in the cerebellum with the levels of *Shh* or the downstream target *Gli1*. Thus, signals other than Shh must also regulate *Mycn* in the developing cerebellum. Consistent with the persistent expression of *Mycn* and *Ccnd1* in our mutants, a proliferating EGL is sustained in *Gli2-En1* cko mice until P8 and until birth in *Smo-Nes* cko mice. Furthermore, cell death is not a contributing factor to the cerebellar phenotypes in *En1-Gli2* cko or *Nes-Smo* cko mutants, as TUNEL assay and immunostaining for activated caspase 3 did not reveal any differences in cell death between wild types and mutants at E18.5 (data not shown). Thus, Shh is clearly required to increase the level of GCP proliferation after E17.5, and to enable the process of foliation.

Shh and formation of more complex cerebella

In this study, we set out to test our prediction that the length and level of Shh signaling determines the extent of foliation in different mammals by controlling the amount of GCP proliferation in specific areas of the cerebellum (Corrales et al., 2004). The genetic mutants we constructed have a graded series of Shh signaling in the postnatal cerebellum, from a complete lack of Shh signaling through upregulated Shh signaling. The resulting cerebellar phenotypes correspondingly progress from no foliation, through immature foliation patterns, to an increased complexity of foliation. The size of the cerebellum also increases in conjunction with a greater elaboration of foliation. Furthermore, the phenotypes correlate with the length of GCP proliferation, their number and the level of *Mycn* transcription in GCPs. Thus, we have demonstrated that the extent of Shh signaling can indeed regulate the extent of foliation in mice.

In all of our mutants, the pattern of foliation reflects the normal progression of fissure formation during mouse development and represents a variation of patterns observed in different organisms. Of likely relevance to this, some of the tertiary fissures in the mouse cerebellum normally form only in certain genetic backgrounds (Inouye and Oda, 1980), and notably they correspond with fissures always present in the rat cerebellum. Furthermore, we found that all but one of these variable fissures are present in transgenic mice with increased Shh signaling (*Shh-P1* mice) and a new fissure forms in a conserved position when signaling is further increased (*Shh-P1;Ptch1*$^{+/-}$ mice). An attractive interpretation of these findings is that the location of fissures is preordained by an as yet to be discovered genetic pathway, and that the number of fissures that form in a particular mammal is determined by the extent of Shh signaling. The level and length of Shh signaling will be determined by many factors, including the number of PCs that are produced, the level of *Shh* transcription in different lobules and expression of factors that enhance or attenuate Shh activity.

We are grateful to Drs G. Fishell, R. Sillitoe and M. Zervas for critical reading of the manuscript, to Dr C. B. Bai for spinal cord analysis of *Gli2*$^{\Delta/\Delta}$ embryos, and to Dr Roy Sillitoe for the rat cerebellum section. We thank Dr A. P. McMahon for providing the *Smo* conditional mutant mice and Kirsten Mimberg for technical assistance. S.B. was partially supported by a post-doctoral fellowship from the DFG. This work was supported by a grant from the NICHD. A.L.J. is a HHMI investigator.

Supplementary material

Supplementary material for this article is available at
http://dev.biologists.org/cgi/content/full/133/9/1811/DC1

References

Altman, J. and Bayer, S. A. (1997). *Development of the Cerebellar System: In Relation to its Evolution, Structure, and Functions*. New York: CRC Press.

Aruga, J., Minowa, O., Yaginuma, H., Kuno, J., Nagai, T., Noda, T. and Mikoshiba, K. (1998). Mouse Zic1 is involved in cerebellar development. *J. Neurosci.* **18**, 284-293.

Auerbach, W., Dunmore, J. H., Fairchild-Huntress, V., Fang, Q., Auerbach, A. B., Huszar, D. and Joyner, A. L. (2000). Establishment and chimera analysis of 129/SvEv- and C57BL/6-derived mouse embryonic stem cell lines. *Biotechniques* **29**, 1024-1032.

Bai, C. B., Auerbach, W., Lee, J. S., Stephen, D. and Joyner, A. L. (2002). Gli2, but not Gli1, is required for initial Shh signaling and ectopic activation of the Shh pathway. *Development* **129**, 4753-4761.

Bai, C. B., Stephen, D. and Joyner, A. L. (2004). All mouse ventral spinal cord patterning by hedgehog is Gli dependent and involves an activator function of Gli3. *Dev. Cell* **6**, 103-115.
Baptista, C. A., Hatten, M. E., Blazeski, R. and Mason, C. A. (1994). Cell-cell interactions influence survival and differentiation of purified Purkinje cells in vitro. *Neuron* **12**, 243-260.
Blaess, S., Corrales, J. D. and Joyner, A. L. (2006). Sonic hedgehog regulates Gli activator and repressor functions with spatial and temporal precision in the mid/hindbrain region. *Development* **133**, 1799-1809.
Caddy, K. W. and Biscoe, T. J. (1979). Structural and quantitative studies on the normal C3H and Lurcher mutant mouse. *Philos. Trans. R. Soc. Lond. B Biol. Sci.* **287**, 167-201.
Ciemerych, M. A., Kenney, A. M., Sicinska, E., Kalaszczynska, I., Bronson, R. T., Rowitch, D. H., Gardner, H. and Sicinski, P. (2002). Development of mice expressing a single D-type cyclin. *Genes Dev.* **16**, 3277-3289.
Corrales, J. D., Rocco, G. L., Blaess, S., Guo, Q. and Joyner, A. L. (2004). Spatial pattern of sonic hedgehog signaling through Gli genes during cerebellum development. *Development* **131**, 5581-5590.
Dahmane, N. and Ruiz-i-Altaba, A. (1999). Sonic hedgehog regulates the growth and patterning of the cerebellum. *Development* **126**, 3089-3100.
Doughty, M. L., Delhaye-Bouchaud, N. and Mariani, J. (1998). Quantitative analysis of cerebellar lobulation in normal and agranular rats. *J. Comp. Neurol.* **399**, 306-320.
Dussault, I., Fawcett, D., Matthyssen, A., Bader, J. A. and Giguere, V. (1998). Orphan nuclear receptor ROR alpha-deficient mice display the cerebellar defects of staggerer. *Mech. Dev.* **70**, 147-153.
Fan, H. and Khavari, P. A. (1999). Sonic hedgehog opposes epithelial cell cycle arrest. *J. Cell Biol.* **147**, 71-76.
Goldowitz, D., Cushing, R. C., Laywell, E., D'Arcangelo, G., Sheldon, M., Sweet, H. O., Davisson, M., Steindler, D. and Curran, T. (1997). Cerebellar disorganization characteristic of reeler in scrambler mutant mice despite presence of reelin. *J. Neurosci.* **17**, 8767-8777.
Goodrich, L. V., Milenkovic, L., Higgins, K. M. and Scott, M. P. (1997). Altered neural cell fates and medulloblastoma in mouse patched mutants. *Science* **277**, 1109-1113.
Graus-Porta, D., Blaess, S., Senften, M., Littlewood-Evans, A., Damsky, C., Huang, Z., Orban, P., Klein, R., Schittny, J. C. and Muller, U. (2001). Beta1-class integrins regulate the development of laminae and folia in the cerebral and cerebellar cortex. *Neuron* **31**, 367-379.
Herrup, K. (1983). Role of staggerer gene in determining cell number in cerebellar cortex. I. Granule cell death is an indirect consequence of staggerer gene action. *Brain Res.* **313**, 267-274.
Inouye, M. and Oda, S. I. (1980). Strain-specific variations in the folial pattern of the mouse cerebellum. *J. Comp. Neurol.* **190**, 357-362.
Ito, M. (1984). *Cerebellum and Neural Control*. New York: Raven Press.
Jacob, J. and Briscoe, J. (2003). Gli proteins and the control of spinal-cord patterning. *EMBO Rep.* **4**, 761-765.
Kenney, A. M. and Rowitch, D. H. (2000). Sonic hedgehog promotes G(1) cyclin expression and sustained cell cycle progression in mammalian neuronal precursors. *Mol. Cell. Biol.* **20**, 9055-9067.
Kenney, A. M., Cole, M. D. and Rowitch, D. H. (2003). Nmyc upregulation by sonic hedgehog signaling promotes proliferation in developing cerebellar granule neuron precursors. *Development* **130**, 15-28.
Kimmel, R. A., Turnbull, D. H., Blanquet, V., Wurst, W., Loomis, C. A. and Joyner, A. L. (2000). Two lineage boundaries coordinate vertebrate apical ectodermal ridge formation. *Genes Dev.* **14**, 1377-1389.
Lauder, J. M., Altman, J. and Krebs, H. (1974). Some mechanisms of cerebellar foliation: effects of early hypo- and hyperthyroidism. *Brain Res.* **76**, 33-40.
Lewis, P. M., Gritli-Linde, A., Smeyne, R., Kottmann, A. and McMahon, A. P. (2004). Sonic hedgehog signaling is required for expansion of granule neuron precursors and patterning of the mouse cerebellum. *Dev. Biol.* **270**, 393-410.
Li, J. Y., Lao, Z. and Joyner, A. L. (2002). Changing requirements for Gbx2 in development of the cerebellum and maintenance of the mid/hindbrain organizer. *Neuron* **36**, 31-43.
Long, F., Zhang, X. M., Karp, S., Yang, Y. and McMahon, A. P. (2001). Genetic manipulation of hedgehog signaling in the endochondral skeleton reveals a direct role in the regulation of chondrocyte proliferation. *Development* **128**, 5099-5108.
Lordkipanidze, T. and Dunaevsky, A. (2005). Purkinje cell dendrites grow in alignment with Bergmann glia. *Glia* **51**, 229-234.
Machold, R., Hayashi, S., Rutlin, M., Muzumdar, M. D., Nery, S., Corbin, J. G., Gritli-Linde, A, Dellovade, T., Porter, J. A., Rubin, L. L., et al. (2003). Sonic hedgehog is required for progenitor cell maintenance in telencephalic stem cell niches. *Neuron* **39**, 937-950.
Machold, R., Hayashi, S., Rutlin, M., Muzumdar, M. D., Nery, S., Corbin, J. G., Gritli-Linde, A, Dellovade, T., Porter, J. A., Rubin, L. L., et al. (2003). Sonic hedgehog is required for progenitor cell maintenance in telencephalic stem cell niches. *Neuron* **39**, 937-950.
Mares, V. and Lodin, Z. (1970). The cellular kinetics of the developing mouse cerebellum. II. The function of the external granular layer in the process of gyrification. *Brain Res.* **23**, 343-352.
Matise, M., Auerbach, W. and Joyner, A. L. (2000). Production of targeted embryonic stem cell clones. In *Gene Targeting: A Practical Approach* (ed. A. L. Joyner), pp. 101-132. New York: Oxford University Press.
Matise, M., Auerbach, W. and Joyner, A. L. (2000). Production of targeted embryonic stem cell clones. In *Gene Targeting: A Practical Approach* (ed. A. L. Joyner), pp. 101-132. New York: Oxford University Press.
Matise, M. P., Epstein, D. J., Park, H. L., Platt, K. A. and Joyner, A. L. (1998). Gli2 is required for induction of floor plate and adjacent cells, but not most ventral neurons in the mouse central nervous system. *Development* **125**, 2759-2770.
Mill, P., Mo, R., Fu, H., Grachtchouk, M., Kim, P. C., Dlugosz, A. A. and Hui, C. C. (2003). Sonic hedgehog-dependent activation of Gli2 is essential for embryonic hair follicle development. *Genes Dev.* **17**, 282-294.
Mill, P., Mo, R., Hu, M. C., Dagnino, L., Rosenblum, N. D. and Hui, C. C. (2005). Shh controls epithelial proliferation via independent pathways that converge on N-Myc. *Dev. Cell* **9**, 293-303.
Mo, R., Freer, A. M., Zinyk, D. L., Crackower, M. A., Michaud, J., Heng, H. H., Chik, K. W., Shi, X. M., Tsui, L. C., Cheng, S. H. et al. (1997). Specific and redundant functions of Gli2 and Gli3 zinc finger genes in skeletal patterning and development. *Development* **124**, 113-123.
Oliver, T. G., Grasfeder, L. L., Carroll, A. L., Kaiser, C., Gillingham, C. L., Lin, S. M., Wickramasinghe, R., Scott, M. P. and Wechsler-Reya, R. J. (2003). Transcriptional profiling of the Sonic hedgehog response: a critical role for N-myc in proliferation of neuronal precursors. *Proc. Natl. Acad. Sci. USA* **100**, 7331-7336.
Palma, V. and Ruiz i Altaba, A. (2004). Hedgehog-GLI signaling regulates the behavior of cells with stem cell properties in the developing neocortex. *Development* **131**, 337-345.
Park, H. L., Bai, C., Platt, K. A., Matise, M. P., Beeghly, A., Hui, C. C., Nakashima, M. and Joyner, A. L. (2000). Mouse Gli1 mutants are viable but have defects in SHH signaling in combination with a Gli2 mutation. *Development* **127**, 1593-1605.
Riccomagno, M. M., Martinu, L., Mulheisen, M., Wu, D. K. and Epstein, D. J. (2002). Specification of the mammalian cochlea is dependent on Sonic hedgehog. *Genes Dev.* **16**, 2365-2378.
Rodriguez, C. I., Buchholz, F., Galloway, J., Sequerra, R., Kasper, J., Ayala, R., Stewart, A. F. and Dymecki, S. M. (2000). High-efficiency deleter mice show that FLPe is an alternative to Cre-loxP. *Nat. Genet.* **25**, 139-140.
Sidman, R. L., Lane, P. W. and Dickie, M. M. (1962). Staggerer, a new mutation in the mouse affecting the cerebellum. *Science* **137**, 610-612.
Smeyne, R. J., Chu, T., Lewin, A., Bian, F., Crisman S. S., Kunsch, C., Lira, S. A. and Oberdick, J. (1995). Local control of granule cell generation by cerebellar Purkinje cells. *Mol. Cell Neurosci.* **6**, 230-251.
Stamataki, D., Ulloa, F., Tsoni, S. V., Mynett, A. and Briscoe, J. (2005). A gradient of Gli activity mediates graded Sonic Hedgehog signaling in the neural tube. *Genes Dev.* **19**, 626-641.
Tronche, F., Kellendonk, C., Kretz, O., Gass, P., Anlag, K., Orban, P. C., Bock, R., Klein, R. and Schutz, G. (1999). Disruption of the glucocorticoid receptor gene in the nervous system results in reduced anxiety. *Nat. Genet.* **23**, 99-103.
Wallace, V. A. (1999). Purkinje-cell-derived Sonic hedgehog regulates granule neuron precursor cell proliferation in the developing mouse cerebellum. *Curr. Biol.* **9**, 445-448.
Wechsler-Reya, R. J. and Scott, M. P. (1999). Control of neuronal precursor proliferation in the cerebellum by Sonic Hedgehog. *Neuron* **22**, 103-114.
Wetts, R. and Herrup, K. (1982). Interaction of granule, Purkinje and inferior olivary neurons in lurcher chimaeric mice. I. Qualitative studies. *J. Embryol. Exp. Morphol.* **68**, 87-98.
Wijgerde, M., McMahon, J. A., Rule, M. and McMahon, A. P. (2002). A direct requirement for Hedgehog signaling for normal specification of all ventral progenitor domains in the presumptive mammalian spinal cord. *Genes Dev.* **16**, 2849-2864.
Yamada, K., Fukaya, M., Shibata, T., Kurihara, H., Tanaka, K., Inoue, Y. and Watanabe, M. (2000). Dynamic transformation of Bergmann glial fibers proceeds in correlation with dendritic outgrowth and synapse formation of cerebellar Purkinje cells. *J. Comp. Neurol.* **418**, 106-120.
Zervas, M., Millet, S., Ahn, S. and Joyner, A. L. (2004). Cell behaviors and genetic lineages of the mesencephalon and rhombomere 1. *Neuron* **43**, 345-357.